Available online at www.sciencedirect.com
ScienceDirect
Ceramics International 38S (2012) S391–S395
CERAMICS INTERNATIONAL
www.elsevier.com/locate/ceramint

Low temperature hydrothermal epitaxy of heteroepitaxial $BiFeO_3$ film

S.H. Han [a,*], C.I. Cheon [b], H.-G. Lee [a], H.-W. Kang [a], H.I. Hwang [c]

[a] *Electronic Materials and Device Research Center, Korea Electronics Technology Institute, Seongnam, Gyeonggi 463-816, South Korea*
[b] *Department of Materials Science and Engineering, Hoseo University, Asan, Chungnam 336-795, South Korea*
[c] *Convergence Components R&D Division, Korea Electronics Technology Institute, Seongnam, Gyeonggi 463-816, South Korea*

Available online 12 May 2011

Abstract

Heteroepitaxial $BiFeO_3$ films were fabricated on a single crystal $SrTiO_3$ substrate by hydrothermal epitaxy. There were two different $BiFeO_3$ layers on the $SrTiO_3$ substrate; first interfacial layer and bulk-like second layer. Microstructure development of the $BiFeO_3$ film was dependent on the precursor concentration, mineralizer concentration, and fill factor of the reaction vessel. This two step growth mechanism was discussed by comparing with earlier reports.

Keywords: A. Films; B. Electron microscopy; B. Microstructure-final; D. Ferrites

1. Introduction

$BiFeO_3$ (BFO) has been attracted a great attention due to its coexistence of ferroelectric and antiferromagnetic order parameter. Recently, there has been renewed interest in BFO due to its very large ferroelectric polarization, increased magnetization, and large magnetoelectric coupling, especially in thin film forms [1,2]. However, incorporation of BFO into device application has been hindered by leakage problems due to defect and nonstoichiometry related issues. Hence, there have been great efforts to enhance the quality of the samples.

BFO thin film has been obtained via vapour phase and chemical solution deposition method [1,3,4]. In these cases, high processing temperature or high annealing temperature (above 600 °C) is required to prepare crystalline films with perovskite structures, so bismuth and oxygen vacancies occur in the thin film. Furthermore, residual thermal stresses, inter-diffusion, and reactions between substrate and film can be generated. Therefore, fabrication method using a low processing temperature has an advantage to reduce imperfections in the films for high-performance engineering applications.

Hydrothermal epitaxy is a technique that uses aqueous chemical reaction to synthesize thin film on structurally similar substrate under an elevated pressure (<15 MPa) and a low temperature (90–200 °C) [5]. Film growth occurs at substantially lower temperatures than vapour methods, which excludes the problems of high processing temperatures and the need for ultrahigh vacuum. Ferroelectric materials, such as $BaTiO_3$, PZT, and $PbTiO_3$ thin films were successfully fabricated on single crystal substrates by hydrothermal epitaxy [5–7]. In the case of BFO, several reports on hydrothermal synthesis of BFO powders appeared in the literature [8–10], indicating potential for hydrothermal epitaxy of BFO films. In this study, heteroepitaxial BFO films were fabricated by hydrothermal epitaxy at 200 °C on a single crystal $SrTiO_3$ (STO) substrate. It was confirmed that there were two kinds of layers; first interfacial layer and bulk-like second layer.

2. Experimental

Heteroepitaxial BFO films were synthesized on a (1 0 0) oriented single-crystal STO substrate (Crystech). As TiO_2-terminated STO substrate is advantageous to enhance epitaxial growth of film [11], as-received STO substrates were etched in buffered NH_4F-HF (BHF) solution for 40 s to make the substrate with TiO_2 termination. Equimolar amounts of $Bi(NO_3)_3{\cdot}5H_2O$ and $Fe(NO_3)_3{\cdot}9H_2O$ powders were added to KOH solution and stirred vigorously for 30 min. The solution was then poured into a 100-ml Teflon-lined stainless autoclave. The concentration of precursor powders varied from 0.0025 to

* Corresponding author. Tel.: +82 31 789 7247; fax: +82 31 789 7249.
E-mail address: shhan@keti.re.kr (S.H. Han).

0272-8842/$36.00
doi:10.1016/j.ceramint.2011.05.018

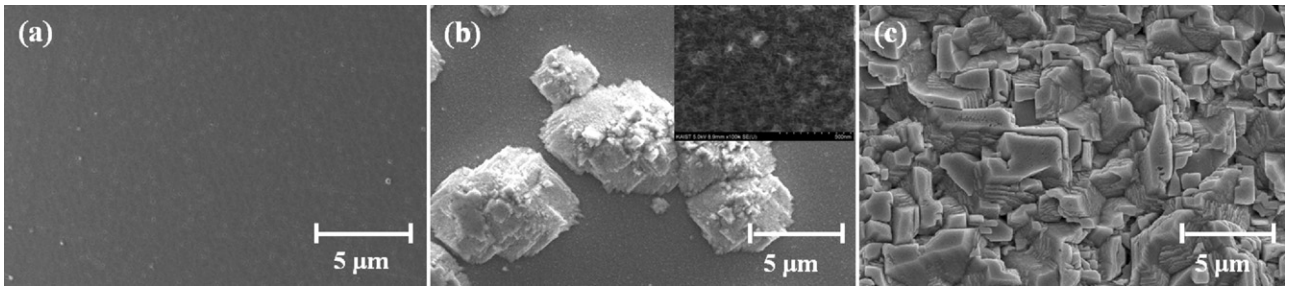

Fig. 1. SEM images of $BiFeO_3$ films fabricated at 200 °C for 10 h with different precursor concentration and fill factor. (a) 0.0025 m, 20%, (b) 0.0025 m, 40%, and (c) 0.005 m, 40%. The inset in (b) is partially enlarged of the first interfacial layer.

0.005 moles, the fill factor of alkaline solution in the Teflon-liner varied from 20% to 40%, and the concentration of KOH varied from 8 M to 16 M. The BHF-treated single-crystal STO substrate was fixed in a Teflon holder with the polished side facing down. The autoclave was placed into a preheated 200 °C oven for 10 h.

The crystal structures and film orientations of the films were analyzed by XRD (Rigaku, D/MAX-RC, λ = 1.5406 Å) using θ–2θ scans over the 2θ range of 15–55°. Identity of the phase was determined by matching the experimental pattern with standards compiled by JCPDS. Microstructural characterizations of the BFO film were performed with SEM (Philips XL30SFEG) and AFM (Seiko SPA400).

3. Results

Perovskite BFO films with different microstructures were synthesized under various synthesis conditions. As shown in Figs. 1 and 5, BFO films with different microstructures were grown on the (1 0 0) STO substrates at various hydrothermal conditions. Fig. 1(a) shows the BFO film synthesized at the precursor concentration of 0.0025 m and the fill factor of 20% (sample 1). The film has smooth and uniform surface. At the higher fill factor of 40% with the same precursor concentration (sample 2), two different layers were formed on the substrate: a first interfacial layer with a acicular shape (inset of Fig. 1(b)) and a second bulk-like layer with a discontinuous pyramid shape (Fig. 1(b)). As precursor concentration increased from 0.0025 to 0.005 m at the 40% fill factor (sample 3), a continuous film with faceted grains crossing at right angle were developed (Fig. 1(c)).

Fig. 2 shows the XRD θ–2θ profiles obtained from the BFO films/STO substrate which were fabricated with various precursor concentrations and fill factors. As shown in Fig. 2(a), perovskite (0 0 1) BFO films were heteroepitaxially grown on a (1 0 0) STO substrate. No other XRD peaks except for those derived from either (1 0 0) STO or (0 0 1) BFO phases were detected. Fig. 2(b) shows the XRD θ–2θ profile around (0 0 2) BFO diffraction peak with intensity in logarithm-scale. XRD peak of sample 1 is different from pristine substrate diffraction peak near 2θ value of about 45° (solid circle). As the precursor concentration and the fill factor increased, strong diffraction peak of $2\theta = 45.9°$ near the substrate peak was newly appeared. This diffraction peak is well consistent with reported bulk BFO value of 45.754° (JCPDS: 86-1518).

The cross-section of sample 2 (Fig. 3(a)) clearly shows the two different layers. The first interfacial layer with thickness of ~80 nm was relatively dense and uniform, but second bulk-like layer has micro-sized pyramid structures. Meanwhile, the cross-section of sample 3 (Fig. 3(b)) shows more a complex pattern with irregular micro-sized grains and non-uniform thickness of 3–4 μm. We could not clearly observe the cross-section of sample 1 due to the low conductivity of substrate and film, and very thin thickness of the film layer.

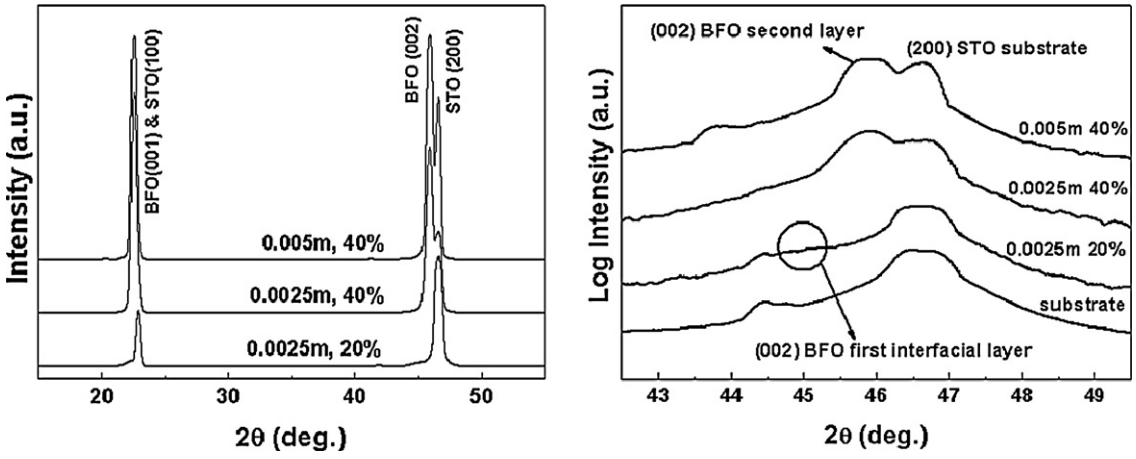

Fig. 2. (a) XRD θ–2θ profiles of $BiFeO_3$ films fabricated at 200 °C for 10 h with different precursor concentration and fill factor. (b) XRD θ–2θ profiles near (0 0 2) $BiFeO_3$ peak with intensity as logarithm-scale.

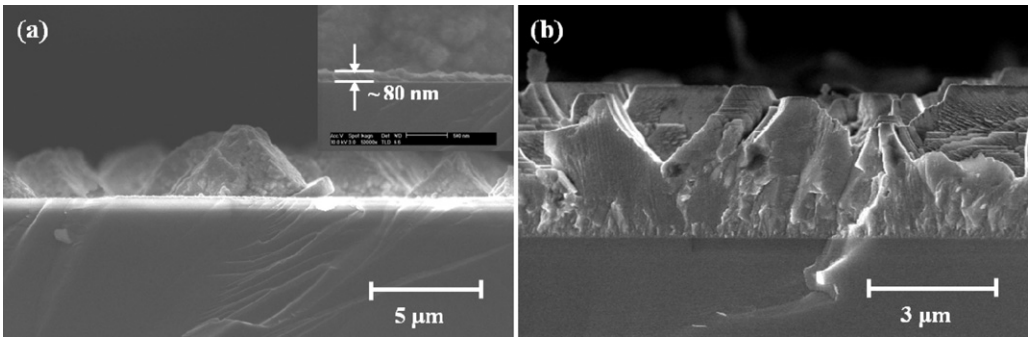

Fig. 3. SEM cross-section images of $BiFeO_3$ films fabricated at 200 °C for 10 h with different precursor concentration and fill factor. (a) 0.0025 m, 40% and (b) 0.005 m, 40%. The inset in (a) is partially enlarged of the first interfacial layer.

In order to observe the surface morphology, AFM observation was carried out for the sample 1 and first interfacial layer of sample 2 (Fig. 4). As shown in Fig. 4(a), surface morphology of sample 1 was very dense and the primary grains were very fine. The root-mean-square (RMS) surface roughness value was ~2.89 nm. On the other hand, surface morphology of the sample 2 had relatively large primary grains compared with sample 1 and the RMS surface roughness value was ~7.11 nm. Increased RMS value may be originated from acicular surface of sample 2.

Influence of mineralizer concentration on the phase formation and microstructure of BFO film was also investigated. Experimental condition was same with sample 1 but only KOH concentration was increased to 12 M and 16 M. As shown in Fig. 5(a) and inset of Fig. 5(a), BFO film fabricated at KOH concentration of 12 M also had two different layers. The first interfacial layer similar with that of sample 2 was formed on the STO substrate, but the second layer was irregular sub-micron sized islands with rounded edge. Thickness of the first layer was ~80 nm (Fig. 5(b)) which is also similar with sample 2 and the second layer was very flat. At the KOH concentration of 16 M (Fig. 5(c) and (d)), film had smooth and uniform thickness but other phases such as potassium bismuth oxide and potassium iron oxide were formed instead of BFO due to the high concentration of KOH (not shown).

4. Discussion

SEM and XRD analyses have confirmed that BFO film was grown on the (1 0 0) STO substrate with two different layers. The epitaxial film was grown at low precursor concentration (0.0025 m), small fill factor (20%), and low mineralizer concentration (8 M KOH). The out-of plane lattice parameter calculated from the (002) peak of sample 1 is ~4.02 Å. This value is larger than the bulk lattice constant (3.96 Å) but very close to that of the BFO epitaxial film grown on the $SrRuO_3$/STO substrate fabricated by pulsed laser deposition (4.00 Å with 200 nm thickness) [1] and metal–organic chemical vapour deposition (4.03 Å with 150 nm thickness) [3]. At higher fill factor, precursor concentration or mineralizer concentration, micro-sized grains were grown on the initial interfacial layer with pyramid shape.

Han et al. [12] showed that PZT film fabricated by hydrothermal epitaxy on the Nb-doped STO substrate consisted of (1 0 0) interfacial layer and (0 0 1) second layer. First interfacial layer was smooth surface and second layer was separated square shape. Heteroepitaxial $KNbO_3$ thin films and nanostructures fabricated by hydrothermal epitaxy on STO substrate also had two different layers: initial coalescent square islands and array of nano-sized tower-like structures [13].

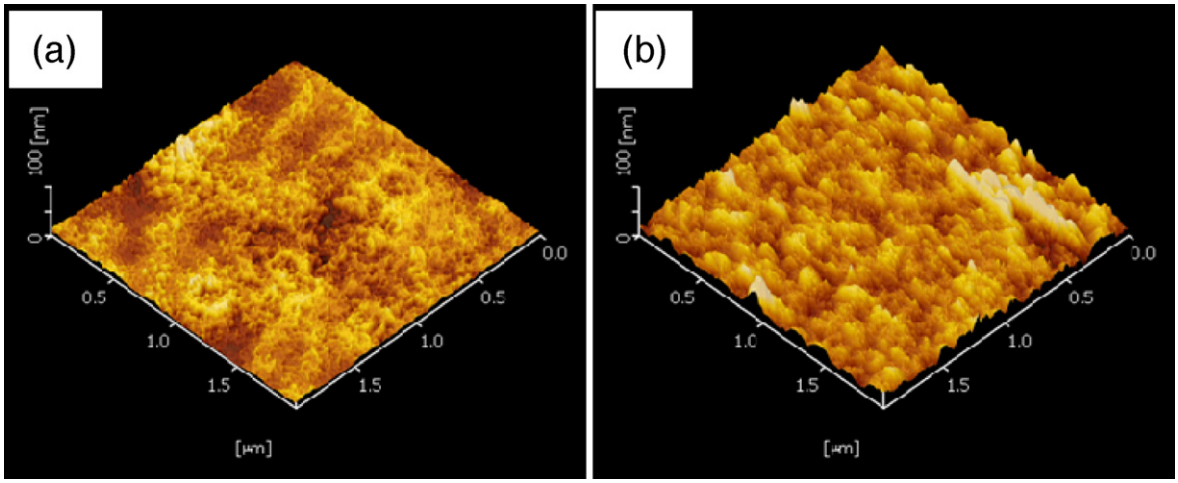

Fig. 4. AFM surface images of $BiFeO_3$ films fabricated at 200 °C for 10 h with different precursor concentration and fill factor. (a) 0.0025 m, 20% and (b) 0.0025 m, 40%. AFM image of (b) is the partial view of the first interfacial layer.

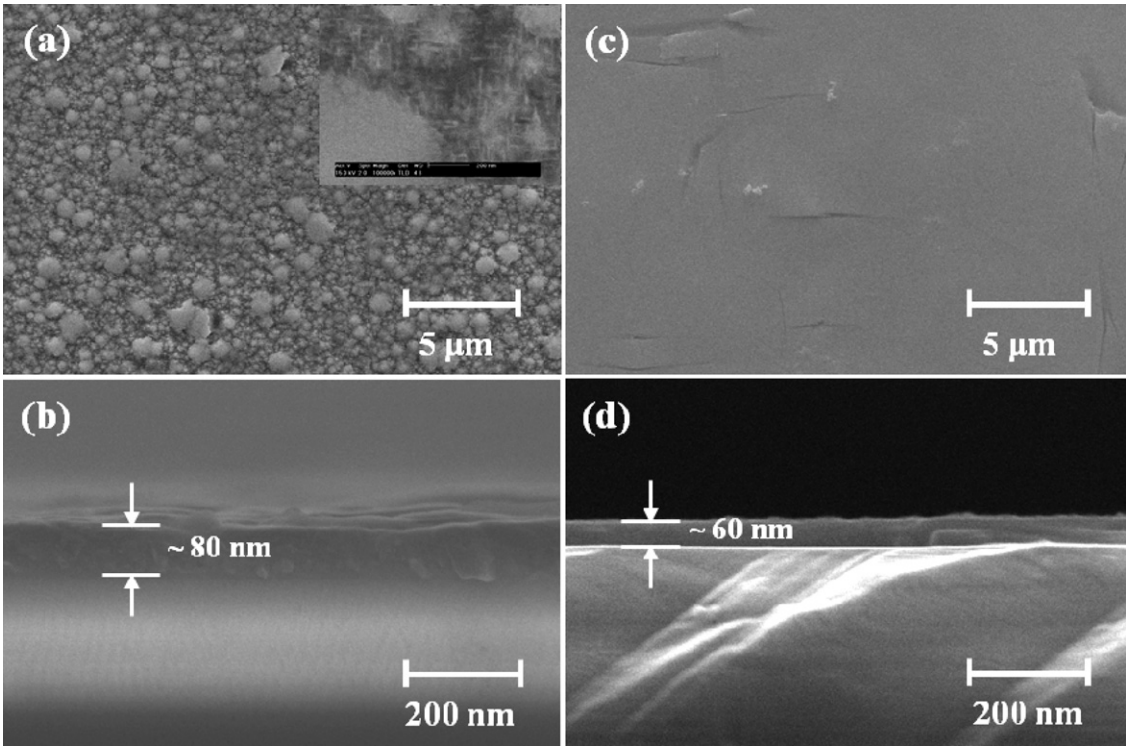

Fig. 5. SEM plane and cross-section images of $BiFeO_3$ films fabricated at 200 °C for 10 h with 0.0025 m precursor concentration, 20% fill factor, and different KOH concentrations (a and b) 12 M KOH, and (c and d) 16 M KOH. The inset in (a) is partially enlarged of the first interfacial layer.

Recently, Rørvik et al. [14] found that $PbTiO_3$ nanorod arrays grown on a STO substrate by hydrothermal synthesis had two step growth mechanism: first thin and dense epitaxial layer was formed on the substrate and then self-assembly of nanocrystals formed a mesocrystal layer which matured into $PbTiO_3$ nanorods on the top part. Rørvik et al. demonstrated the nucleation of crystalline $PbTiO_3$ in the dispersion by a LaMer–Dinegar diagram [15].

Generally, the precursor particles dissolve into ions at the high temperature and pressure in hydrothermal synthesis and the ion concentration in the alkali solution increase continuously. When the ion concentration reaches to the saturation point, thermodynamically stable precipitate can grow but the nucleation needs further increase in the degree of supersaturation. The ion concentration increases to a critical value, the precipitate can be nucleated and grown. The nucleation and growth rate depend on the degree of supersaturation. In hydrothermal reaction, the degree of supersaturation increases with the increase in precursor concentration, pressure, or alkali mineralizer concentration at the constant temperature.

When the hydrothermal reaction occurred at low precursor concentration (0.0025 m), small fill factor (20%), and low mineralizer concentration (8 M KOH) in this work, the ion concentration in the solution was higher than the saturation value but low for the nucleation. The low degree of saturation resulted in the dense epitaxial thin film as shown in Fig. 1(a). When the fill factor or the mineralizer concentration increased to 40% or 12 M, respectively, the higher degree of supersaturation led to epitaxial layer and micron-sized BFO islands as shown in Figs. 1(b), 3(a), and 5(a) and (c). The simultaneous increase in the fill factor (40%) and precursor concentration (0.005 m) increased the degree of supersaturation further in the sample 3. The continuous thick film with the complex pattern shown in Figs. 1(c) and 3(b) was formed due to numerous nucleation and higher growth rate. By adjusting the supersaturation more precisely, high quality heteroepitaxial BFO thin film can be grown on the STO substrate. The characteristic of the two different BFO layers is being evaluated.

We observed the pyramid growth of micro-sized islands on the epitaxial dense layer by top and cross-section view of sample 2 (Figs. 1(b) and 3(a)). This kind of pyramid structure was also observed on the $PbTiO_3$ micro-island fabricated by hydrothermal epitaxy [16]. After atomically smooth islands were formed on the STO substrate, pyramid structure was developed on the island due to the presence of spiral dislocation on the island surface. In the case STO substrate with ~1 μm terrace width, the critical film thickness to form pyramid structure was ~70 nm. Because we also used substrate with ~1 μm terrace width and film thickness of BFO was ~80 nm, pyramid structure might be formed from spiral dislocation. Further studies are needed to understand the formation mechanism of spiral dislocation on the epitaxial BFO film.

5. Conclusion

We fabricated heteroepitaxial BFO films on a single crystal STO substrate by hydrothermal epitaxy. The very thin BFO film with smooth surface was grown at low precursor concentration and fill factor. The discontinuous micron-sized BFO islands

were formed over the initially grown interfacial layer at the higher fill factor. And the rough continuous film with faceted grains was developed at the high precursor concentration and fill factor. Increasing mineralizer concentration caused submicron sized islands with rounded edge on the first interfacial layer. Microstructure development of the BFO thin film was dependent on the degree of supersaturation.

Acknowledgement

This work was supported by a Grant from Fundamental R&D Program for Core Technology of Materials funded by the Ministry of Knowledge Economy, Republic of Korea.

References

[1] J. Wang, J.B. Neaton, H. Zheng, V. Nagarajan, S.B. Ogale, B. Liu, D. Viehland, V. Vaithyanathan, D.G. Schlom, U.V. Waghmare, N.A. Spaldin, K.M. Rabe, M. Wuttig, R. Ramesh, Epitaxial $BiFeO_3$ multiferroic thin film heterostructures, Science 299 (2003) 1719–1722.

[2] W. Eerenstein, F.D. Morrison, J. Dho, M.G. Blamire, J.F. Scott, N.D. Mathur, Comment on epitaxial $BiFeO_3$ multiferroic thin film heterostructures, Science 307 (2005) 1203a.

[3] S.Y. Yang, F. Zavaliche, L. Mohaddes-Ardabili, V. Vaithyanathan, D.G. Schlom, Y.J. Lee, Y.H. Chu, M.P. Cruz, Q. Zhan, T. Zhao, R. Ramesh, Metalorganic chemical vapour deposition of lead-free ferroelectric $BiFeO_3$ films for memory applications, Applied Physics Letters 87 (2005) 102903.

[4] A.H.M. Gonzalez, A.Z. Simoes, L.S. Cavalcante, E. Longo, J.A. Varela, C.S. Riccardi, Soft chemical deposition of $BiFeO_3$ multiferroic thin films, Applied Physics Letters 90 (2007) 052906.

[5] A.T. Chien, L. Zhao, M. Colic, J.S. Speck, F.F. Lange, Microstructural development of $BaTiO_3$ heteroepitaxial thin films by hydrothermal synthesis, Journal of Materials Research 13 (1998) 649–659.

[6] W.S. Ahn, W.W. Jung, S.K. Choi, Ferroelectric properties and fatigue behaviour of heteroepitaxial $PbZr_{1-x}Ti_xO_3$ thin film fabricated by hydrothermal epitaxy below Curie temperature, Journal of Applied Physics 99 (2006) 014103.

[7] A.T. Chien, J. Sachleben, J.H. Kim, J.S. Speck, F.F. Lange, Synthesis and characterization of $PbTiO_3$ powders and heteroepitaxial thin films by hydrothermal synthesis, Journal of Materials Research 14 (1999) 3303–3311.

[8] C. Chen, J. Cheng, S. Yu, L. Che, Z. Meng, Hydrothermal synthesis of perovskite bismuth ferrite crystallites, Journal of Crystal Growth 292 (2006) 135–139.

[9] J.T. Han, Y.H. Huang, X.J. Wu, C.L. Wu, W. Wei, B. Peng, W. Huang, J.B. Goodenough, Tunable synthesis of bismuth ferrites with various morphologies, Advanced Materials 18 (2006) 2145–2148.

[10] Y. Wang, G. Xu, Z. Ren, X. Wei, W. Weng, P. Du, G. Shen, G. Han, Mineralizer-assisted hydrothermal synthesis and characterization of $BiFeO_3$ nanoparticles, Journal of the American Ceramic Society 90 (2007) 2615–2617.

[11] M. Kawasaki, K. Takahashi, T. Maeda, R. Tsuchiya, M. Shinohara, O. Ishiyama, T. Yonezawa, M. Yoshimoto, H. Koinuma, Atomic control of the $SrTiO_3$ crystal surface, Science 266 (1994) 1540–1542.

[12] S.H. Han, W.S. Ahn, H.C. Lee, S.K. Choi, Ferroelectric properties of heteroepitaxial $PbTiO_3$ and $PbZr_{1-x}Ti_xO_3$ films on Nb-doped $SrTiO_3$ fabricated by hydrothermal epitaxy below Curie temperature, Journal of Materials Research 22 (2007) 1037–1042.

[13] G.K.L. Goh, C.G. Levi, J.H. Choi, F.F. Lange, Hydrothermal epitaxy of $KNbO_3$ thin films and nanostructures, Journal of Crystal Growth 286 (2006) 457–464.

[14] P.M. Rørvik, Å. Almli, A.T.J. van Helvoort, R. Holmestad, T. Tybell, T. Grande, M.A. Einarsrud, $PbTiO_3$ nanorod arrays grown by self-assembly of nanocrystals, Nanotechnology 19 (2008) 225605.

[15] V.K. LaMer, R.H. Dinegar, Theory, production and mechanism of formation of monodispersed hydrosols, Journal of the American Chemical Society 72 (1950) 4847–4854.

[16] J.H. Jeon, S.K. Choi, Growth mode transition to pyramid from layer by layer of heteroepitaxial PbTiO3 islands on a (0 0 1) vicinal SrTiO3 substrate fabricated by hydrothermal epitaxy, Applied Physics Letters 91 (2007) 091916.